

Determination of a quantitative criterion to distinguish between coherent and incoherent approaches in the thermometric interpretation of Coherent anti-Stokes Raman spectra

M. Marrocco

ENEA, via Anguillarese 301, 00060 Santa Maria di Galeria (Rome), Italy

ABSTRACT

Coherent anti-Stokes Raman spectroscopy (CARS) is an important spectroscopic technique that has large application in thermometry of hostile environments (jet engines, internal combustion engines, coal gasifiers, furnaces, flames, and so on). It is based on the use of three laser systems and the achievement of a high precision relies on the best spectral convolution over the relevant bandwidths when degeneracy of laser frequencies is involved. Although analytical solutions of CARS signals generated by pump and Stokes lasers with standard (i.e. gaussian or lorentzian) lineshapes are well known, research in this field has overlooked the criterion on how to discern coherence between spectral components of the third-order non-linear susceptibility that characterizes the optical response of the medium. Understandably, the ordinary approach is based on an intuitive comparison between the spectral width σ_1 of the pump laser with respect to the width Γ of the relevant Raman transitions. More precisely, if $\sigma_1 \ll \Gamma$ then the spectral synthesis can be obtained in the limit of narrowband pump, otherwise spectral coherence has to be included in the calculation leading up to problematic spectral analysis. In an attempt to better clarify this qualitative criterion, the present work demonstrates that the limit between the two opposite regimes can have a clearer and neater definition than that accepted so far. In this case, this work shows that the issue is governed by the analytic function $\rho_{\text{on}} = \sqrt{\pi} \Gamma \exp[(\Gamma/\sigma_1)^2] \text{erfc}(\Gamma/\sigma_1)/\sigma_1$ which depends uniquely on the ratio Γ/σ_1 . The unitary limit of this function for $\sigma_1 \ll \Gamma$ justify the incoherent or the narrowband-pump approach.

1. INTRODUCTION

Coherent Anti-Stokes Raman Spectroscopy (CARS) is a mature spectroscopic technique based on wave mixing of electromagnetic fields through the third-order nonlinear optical susceptibility.¹⁻⁵ It was first introduced by Maker and Terhune forty years ago,⁶ and, after their pioneering work, a large number of authors has illustrated the potential of CARS as an important approach for high-resolution molecular spectroscopy.¹⁻⁵ This abundant research on the physical basics of such a fundamental nonlinear process has yielded a flourishing literature on different applicative examples, and, among them, thermometry. It is, indeed, widely accepted that CARS is at present the most effective strategy for remote sensing of temperature in hostile environments such as plasmas, flames, combustion engines, and exhaust from jet engines.¹⁻⁵

The detailed interpretation of spectral shapes of CARS measurements is faced in a rather limited number of published works,⁷⁻¹³ which illustrate the impact of finite laser bandwidths on CARS accuracy and reliability. The problem traces back to a famous work of Yuratich,⁷ where a simple incoherent convolution over the laser bandwidths had been suggested. Later, other authors questioned Yuratich's work by showing that more complex convolutions were necessary to account for interferences between the spectral components of $\chi^{(3)}$.⁸⁻¹¹ Right after these findings, multimode laser operation, resulting in gaussian spectral profiles, was included in the analytical calculation of anti-Stokes signals^{12, 13} and the whole issue was organized into a computational tool.¹⁴ Since then, many authors have relied on these achievements to classify the operative conditions under which CARS theory brings off the correct data explanation.¹⁵⁻³²

In this paper, the focus is on the criterion of applicability of standard approaches based on Yuratich's⁷ and other authors'⁸⁻¹⁴ analysis. At present, the general criterion to discriminate between them is rather loose in the sense that incoherent convolution (i.e. Yuratich approach) is accepted only if the spectral width of the pump lasers is much smaller than the width Γ of the relevant Raman transitions.^{1, 8-14} Surprisingly, no one has ever investigated the question of whether or not it is possible to better define the imprecise inequality expressed by the words "much smaller" and, put differently, we can ask ourselves if there exist a more precise reasoning that could act as yardstick to measure the relevance of coherent convolution in the calculation of CARS.

The paper is organized as follows. The basic notation of this work, as well as some introductory notes on the subject, is set out in the second section. The standard approach with gaussian spectral profiles of the three laser beams is revised in the third section. It must be observed that even though the revision might be regarded as a repetition of published results, it will include the more general notation for non-degenerate pump beams. Degeneracy, useful for comparisons with the known expressions of Ref. 13, will be pursued by equaling the parameters of the two pump lasers. After these preparatory sections, the most interesting part of this work is in the fourth section, where the quantitative criterion to discriminate between incoherent and coherent convolutions will be laid out. Conclusions are in the final section.

2. NOTATION

The CARS signal I_{CARS} is traditionally written as a simple combination of two degenerate monochromatic pump lasers $L_1(\bar{\omega}_1) = L_2(\bar{\omega}_2)$ (with $\bar{\omega}_1 = \bar{\omega}_2$) and a broadband Stokes laser $L_S(\omega_S)$,

$$I_{CARS}(\omega_a) = K |\chi(\bar{\omega}_1 - \omega_S)|^2 [L_1(\bar{\omega}_1)]^2 L_S(\omega_S) \quad (1)$$

where K is a proportionality constant and χ is the non-linear susceptibility depending on the frequency difference $\bar{\omega}_1 - \omega_S$ between the fixed pump frequency $\bar{\omega}_1$ and the Stokes frequency ω_S [note that in Eq. (1) we have suppressed the superscript (3) of χ for simplicity]. Since the monochromaticity of L_1 , $\bar{\omega}_1$ cannot be varied and the anti-Stokes signal I_{CARS} at frequency ω_a is solely determined by the Stokes laser intensity $L_S(\omega_S)$ at frequency $\omega_S = 2\bar{\omega}_1 - \omega_a$. Unfortunately, this situation holds only for some rather sophisticated pump lasers (for instance, injection-seeded Nd:YAG lasers) whose bandwidth is about one order of magnitude smaller than the linewidth of the Raman resonances.³³ More generally, pump lasers employed in CARS measurements have a finite linewidth,^{1, 8-14} which is comparable or larger than the Raman widths.^{15-18, 20-21, 23, 24, 26, 28-32} In this case, one should transform Eq. (1) into an intuitive spectral convolution over the three laser profiles,

$$I_{CARS}(\omega_a) = K \int |\chi(\omega_1 - \omega_S)|^2 L_1(\omega_1) L_2(\omega_2) L_S(\omega_S) \delta(\omega_1 + \omega_2 - \omega_S - \omega_a) d\omega_1 d\omega_2 d\omega_S \quad (2)$$

where the two pump lasers are now supposed non-degenerate, and the δ function guarantees the energy conservation. Note that, with this generalization, En. (1) can be viewed as the limit of En. (2) for degenerate pump lasers having very small linewidths σ_1 and σ_2 .

Equation (2) was commonly used in early CARS studies.³⁴⁻³⁶ But, it was soon realized that interferences among the different spectral components of χ had a relevant contribution to the CARS signal and a more complex convolution was introduced to accurately interpret CARS measurements,^{8, 10}

$$I_{CARS}(\omega_a) = K \int |\chi_{12S}|^2 L_1(\omega_1) L_2(\omega_2) L_S(\omega_S) \delta(\omega_1 + \omega_2 - \omega_S - \omega_a) d\omega_1 d\omega_2 d\omega_S \quad (3)$$

where

$$\chi_{12S} = \chi_{NR} + \frac{1}{2}\chi_{1S}(\omega_1 - \omega_S) + \frac{1}{2}\chi_{2S}(\omega_2 - \omega_S). \quad (4)$$

The first term on the right-hand side of En. (4) is the so-called non-resonant susceptibility and takes into account the background due to the Raman-inactive medium. The other two terms give off the relevant CARS signal, which, besides the multiplicity of vibrational-rotational Raman transitions, incorporates coherent phenomena between the spectral components accessed by $\omega_1 - \omega_S$ and $\omega_2 - \omega_S$.

As will become apparent shortly, the calculation of En. (3) is fundamental to the argument of this paper. To that end, the customary method of working out a solution of $I_{CARS}(\omega_a)$ is to break it up into four different pieces indicated below

$$I_1 = K\chi_{NR}^2 \int L_1(\omega_1)L_2(\omega_2)L_S(\omega_S)\delta(\omega_1 + \omega_2 - \omega_S - \omega_a)d\omega_1d\omega_2d\omega_S \quad (5)$$

$$I_2 = \frac{1}{2}K\chi_{NR} \int (\chi_{1S} + \chi_{2S} + \chi_{1S}^* + \chi_{2S}^*)L_1(\omega_1)L_2(\omega_2)L_S(\omega_S)\delta(\omega_1 + \omega_2 - \omega_S - \omega_a)d\omega_1d\omega_2d\omega_S \quad (6)$$

$$I_3 = \frac{1}{4}K \int (\chi_{1S}\chi_{1S}^* + \chi_{2S}\chi_{2S}^*)L_1(\omega_1)L_2(\omega_2)L_S(\omega_S)\delta(\omega_1 + \omega_2 - \omega_S - \omega_a)d\omega_1d\omega_2d\omega_S \quad (7)$$

$$I_4 = \frac{1}{4}K \int (\chi_{1S}\chi_{2S}^* + \chi_{1S}^*\chi_{2S})L_1(\omega_1)L_2(\omega_2)L_S(\omega_S)\delta(\omega_1 + \omega_2 - \omega_S - \omega_a)d\omega_1d\omega_2d\omega_S \quad (8)$$

where the asterisk stands for complex conjugate and χ_{pS} (with $p = 1, 2$) is given by a summation running over the possible Raman transitions

$$\chi_{pS}(\omega_p - \omega_S) = \sum_j a_j \frac{1}{\Omega_j - (\omega_p - \omega_S) - i\Gamma_j}. \quad (9)$$

In En. (9), the Raman frequencies and linewidths (namely the half widths at half height) are respectively indicated as Ω_j and Γ_j . The factor a_j denotes the strength of the associated transition and takes in the dependences on the population difference and the Raman cross-section. The explicit expressions of Ω_j , Γ_j and a_j can be found in many works^{1, 3-5, 8, 14, 34} and, for this reason, are not given in this context.

3. CALCULATION OF CARS SIGNALS WITH GAUSSIAN LASER PROFILES

To put the whole issue into perspective, we begin with the revision of the classical result obtained with degenerate gaussian pump laser profiles.¹³ The alternative of lorentzian bandwidths will not be considered here. This is in line with the fact that the gaussian dependence is more appropriate for most of the laser systems employed in CARS measurements. It is known, indeed, that these lasers possess inhomogeneously broadened lines, which, with a good level of approximation, result in gaussian shapes.³⁷

After such a preliminary but necessary remark, a second resolution of this work is that, unlike the common tendency to calculate spectral convolutions of degenerate pump lasers, the following calculations will be as general as possible. Degeneracy will be reintroduced only when the comparison with the result of Yueh and Beiting¹³ is invoked.

The gaussian dependence of the pump and Stokes lasers is then assumed to be

$$L_p(\omega_p) = \frac{L_p}{\sqrt{\pi}\sigma_p} \exp[-(\omega_p - \bar{\omega}_p)^2/\sigma_p^2], \quad (10)$$

with $p = 1, 2$ or S . In En. (10), $\bar{\omega}_p$ indicates the central frequency, $\sigma_p = \bar{\sigma}_p / b$ the normalized half width with $\bar{\sigma}_p$ the actual half width and b a constant depending on the definition of $\bar{\sigma}_p$ (i.e. $b = \sqrt{2}$ or $\sqrt{\ln 2}$). Note that, if L_p indicates the laser intensity, then $L_p(\omega_p)$ has the physical dimension of spectral intensity.

All the essential information needed to undertake the calculation of the total CARS signal I_{CARS} of gaussian profiles has been brought out and we are now ready to move on to the revision of the standard approach summarized in the results of Ref. 13. To help the reader follow the progression of this work as carefully as possible, the calculation has been divided into four different steps, each one related to a term into which the CARS signal has been split up [see Eqs. (5)-(8)].

3.1 Calculation of I_1 for gaussian profiles

The calculation of En. (5) is very simple. We can first eliminate the δ function by putting $\omega_1 = \omega_a + \omega_S - \omega_2$ and then solve the remaining integrals of gaussian functions. After some manipulation, the result is

$$I_{1g} = K\chi_{NR}^2 L_1 L_2 L_S \frac{1}{\sqrt{\pi}\sigma_{12S}} \exp[-(\omega_a - \bar{\omega}_a)^2 / \sigma_{12S}^2] \quad (11)$$

where the subscript g refers to the gaussian profiles, $\bar{\omega}_a = \bar{\omega}_1 + \bar{\omega}_2 - \bar{\omega}_S$ and $\sigma_{12S} = \sqrt{\sigma_1^2 + \sigma_2^2 + \sigma_S^2}$. The term I_{1g} is featureless in that no Raman resonances take place, and, as long as $\sigma_S \gg \sigma_1, \sigma_2$, valid for broadband CARS, the sole noteworthy aspect of I_{1g} is in the reproduction of the spectral profile of the Stokes laser.

Comparison with the result of Yueh and Beiting¹³ is soon established once we put $\bar{\omega}_1 = \bar{\omega}_2$ and $\sigma_1 = \sigma_2$ in En. (11). It is then straightforward to verify a complete agreement with the term $A\chi_{NR}^2$ of Ref. 13 relative to gaussian laser lineshapes.

3.2 Calculation of I_2 for gaussian profiles

The simplicity seen in the calculation of Eq. (5) does not recur in En. (6). However, the difficulties inherent in the treatment of I_2 are more readily handled if we first consider one of its pieces, that is

$$I_2^{1S} = \frac{1}{2} K\chi_{NR} \int (\chi_{1S} + \chi_{1S}^*) L_1(\omega_1) L_2(\omega_2) L_S(\omega_S) \delta(\omega_1 + \omega_2 - \omega_S - \omega_a) d\omega_1 d\omega_2 d\omega_S. \quad (12)$$

For instance, the δ function can be removed by considering $\omega_1 = \omega_a + \omega_S - \omega_2$. This choice is fortunate in that the remaining gaussian integral with respect to ω_S is easily solved. Nonetheless, the final integral with respect to ω_2 can only be solved with the help of the integration of functions of complex variables. We find

$$I_{2g}^{1S} = -K\chi_{NR} L_1 L_2 L_S \frac{1}{\sigma_2 \sqrt{\sigma_1^2 + \sigma_S^2}} \exp[-(\omega_a - \bar{\omega}_a)^2 / \sigma_{12S}^2] \sum_j a_j \text{Im}[w(z_j)], \quad (13)$$

where

$$z_j = \frac{\sigma_{12S}}{\sigma_2 \sqrt{\sigma_1^2 + \sigma_S^2}} \left[\frac{\sigma_1^2 + \sigma_S^2}{\sigma_{12S}^2} (\omega_a - \bar{\omega}_a) - \Omega_j + \bar{\omega}_1 - \bar{\omega}_S + i\Gamma_j \right] \quad (14)$$

and $w(z_j) = \exp(-z_j^2)\text{erfc}(-iz_j)$ is the complex error function.³⁸ To complete the solution of Eq. (6), it is enough to exchange the indexes 1 and 2 on the right-hand sides of Eqs. (13) and (14). If we call I_{2g}^{2S} the new result, then the solution of Eq. (6) can be written as $I_{2g} = I_{2g}^{1S} + I_{2g}^{2S}$.

The comparison with Ref. 13 is made once we insert the degeneracy ($\bar{\omega}_1 = \bar{\omega}_2$ and $\sigma_1 = \sigma_2$). We find the same expression except for a detail in Eq. (14). According to the work of Yueh and Beiting, the square root of $\sigma_1^2 + \sigma_S^2$ should be replaced by σ_S . This is not a great difference, because $\sigma_S \gg \sigma_1$ for broadband CARS, but it might be of some importance for scanning CARS. Probably, the negligible mistake is due to a misprint that is absent in other authors^{16, 20}, where the results of Ref. 13 have been explicitly mentioned.

3.3 Calculation of I_3 for gaussian profiles

If the results given in Eq. (11) and (13) are decisive to decipher the spectral influence of the non-resonant susceptibility, the next two calculations of I_3 and I_4 provide the more important information carrying the distinctive CARS signatures of the probed molecular species. We begin with I_3 which, between the two, bears the most significant contribution to the Raman resonances that characterize a typical CARS spectrum.

The calculation follows the same logic described above. First of all, we take $\omega_S = \omega_1 + \omega_2 - \omega_a$ by means of the δ function and, then, we are able to split I_3 into two different terms, $I_3 = I_3^{1S} + I_3^{2S}$, where

$$I_3^{1S} = \frac{1}{4} K \int |\chi_{1S}(\omega_a - \omega_2)|^2 L_1(\omega_1) L_2(\omega_2) L_S(\omega_1 + \omega_2 - \omega_a) d\omega_1 d\omega_2, \quad (15)$$

$$I_3^{2S} = \frac{1}{4} K \int |\chi_{2S}(\omega_a - \omega_1)|^2 L_1(\omega_1) L_2(\omega_2) L_S(\omega_1 + \omega_2 - \omega_a) d\omega_1 d\omega_2. \quad (16)$$

Note that Eq. (16) can be deduced from Eq. (15), and viceversa, by swapping over the indexes 1 and 2. This means that the calculation can be limited to I_3^{1S} only.

After the gaussian integral with respect to ω_1 , the remaining integral is solved in terms of the complex error function $w(z_j)$,³⁸

$$I_{3g}^{1S} = -\frac{1}{2} K L_1 L_2 L_S \frac{1}{\sigma_2 \sqrt{\sigma_1^2 + \sigma_S^2}} \exp[-(\omega_a - \bar{\omega}_a)^2 / \sigma_{12S}^2] \sum_{j,m} a_j a_m \text{Im}\{w(z_j) / [\Omega_m - \Omega_j + i(\Gamma_j + \Gamma_m)]\}. \quad (17)$$

Equation (17) is very important as it contains the most striking characteristics of CARS spectra determined by the imaginary part of $w(z_j) / [\Omega_m - \Omega_j + i(\Gamma_j + \Gamma_m)]$. If specified further, this quantity becomes

$$\text{Im}\{w(z_j) / [\Omega_m - \Omega_j + i(\Gamma_j + \Gamma_m)]\} = \frac{(\Omega_m - \Omega_j) \text{Im}[w(z_j)] - (\Gamma_j + \Gamma_m) \text{Re}[w(z_j)]}{(\Omega_m - \Omega_j)^2 + (\Gamma_j + \Gamma_m)^2}, \quad (18)$$

where $\text{Re}[w(z_j)]$ is the well known Voigt profile associated to the j -th Raman resonance. Equation (18) demonstrates that the spectral peaks of CARS measurements are not purely represented by the Voigt profile, unless they are largely spaced. Indeed, if the Raman resonances lie far apart from each other, the overlap can be neglected and the terms for $j \neq m$ can be discarded. In this case, $\text{Im}[w(z_j)]$ does not significantly contribute to the summation of Eq. (17). On the

contrary, when there is some overlap, $\text{Im}[w(z_j)]$ might have a meaningful contribution and the resultant profile differs from the Voigt function $\text{Re}[w(z_j)]$.

At a first look, comparison between the degenerate gaussian expression of $I_{3g} = I_{3g}^{1S} + I_{3g}^{2S}$ and the corresponding result of Ref. 13 might suggest some doubts (in Ref. 13, the complex error function appears with its complex conjugate). But after some simple algebra, the two results are identical [apart from the little detail in Eq. (14) explained before].

3.4 Calculation of I_4 for gaussian profiles

As anticipated by the formal expression of Eq. (8), the calculation of I_4 is useful to ascertain interference effects between the spectral components χ_{1S} and χ_{2S} of the total susceptibility depending on the two frequency differences $\omega_1 - \omega_S$ and $\omega_2 - \omega_S$. But, despite its importance, I_4 cannot be easily calculated. For instance, different authors have commented on the impossibility of solving Eq. (8) with analytical methods when the three gaussian profiles of the lasers are taken into consideration.^{8, 13} However there exist a clever reasoning of Yueh and Beiting¹³ that leads up to a credible result.

According to the prescription, the initial hypothesis of a gaussian Stokes laser is weakened and a constant distribution is assumed instead. In this way, the integrals in I_4 can be fully carried out. Restoring the gaussian dependence will then be a matter of a later substitution based on what transformations would have been applied to I_2 and I_3 if the corresponding Eqs. (6) and (7) had been calculated for a flat Stokes laser.

We begin assuming a constant $L_S(\omega_S) = \bar{L}_S$ in Eq. (8) and then proceed to remove the integral with respect ω_S by taking $\omega_S = \omega_1 + \omega_2 - \omega_a$. Two simple integrals of gaussian functions can be isolated and the overall solution is then

$$I_{4c} = \frac{1}{2} KL_1 L_2 \bar{L}_S \frac{\pi}{\sigma_1 \sigma_2} \sum_{j,m} a_j a_m \{ \text{Re}[w(z_{1,m})] \text{Re}[w(z_{2,j})] + \text{Im}[w(z_{1,j})] \text{Im}[w(z_{2,m})] \}, \quad (19)$$

where

$$z_{p,j} = (\omega_a - \bar{\omega}_p - \Omega_j + i\Gamma_j) / \sigma_p \quad \text{with } p = 1, 2 \quad (20)$$

and the subscript c in I_{4c} refers to the constant Stokes profile. According to the comparison of Eqs. (13) and (17) with what would have been the result of I_2 and I_3 without the Stokes gaussian dependence, restoring the original gaussian $L_S(\omega_S)$ means to consider the following expression

$$I_{4g} = \frac{1}{2} KL_1 L_2 L_S \frac{\sqrt{\pi}}{\sigma_1 \sigma_2 \sqrt{\sigma_1^2 + \sigma_S^2}} \exp[-(\omega_a - \bar{\omega}_a)^2 / \sigma_{12S}^2] \sum_{j,m} a_j a_m \{ \text{Re}[w(z'_{1,m})] \text{Re}[w(z'_{2,j})] + \text{Im}[w(z'_{1,j})] \text{Im}[w(z'_{2,m})] \}, \quad (21)$$

where

$$z'_{1,j} = \frac{\sigma_{12S}}{\sigma_2 \sqrt{\sigma_1^2 + \sigma_S^2}} \left[\frac{\sigma_1^2 + \sigma_S^2}{\sigma_{12S}^2} (\omega_a - \bar{\omega}_a) - \Omega_j + \bar{\omega}_1 - \bar{\omega}_S + i\Gamma_j \right] \quad (22)$$

and $z'_{2,j}$ is obtained by exchanging the indexes 1 and 2 on the right-hand side. However, if the different meaning of the two indexes 1 and 2 is removed, then the degenerate result of Ref. 13 is obtained. An important point that it is worthy of note is that both Eqs. (19) and (21) depend on the summation of products of real and imaginary parts of the complex error function. These products are significant for $m = j$ if the Raman transitions are well separated. But, for closely

spaced resonances, the cross terms become important too. Once again, the real part of the complex error function w gives the Voigt profile and therefore Eq. (21) says that I_{4g} is given by the product of the Voigt profiles plus a slight correction due to the imaginary part of the complex error function w .

4. THE QUANTITATIVE CRITERION

Having given the formal background of the calculation of I_{CARS} , it is now instructive to compare I_{3g} with I_{4g} . The reason of this interest lies in the fact that we are concerned with the appearance of coherence between the components of the third-order susceptibility written in Eq. (4). For this reason, it is indispensable to focus on those integrals where interferences are readily manifest, that is the third and fourth integral previously calculated. It is, indeed, straightforward to understand that the key quantity to evaluate the real impact of coherence between the spectral components of the CARS susceptibility is the ratio between I_{4g} and I_{3g} . However, to gain a more general insight into this specific problem, let us initially consider the ratio ρ between the more general intensities I_4 and I_3 , respectively given in Eqs. (8) and (7). First of all, we note that, if the two susceptibility components χ_{1S} and χ_{2S} in Eq. (4) are independently convolved, then I_4 equals I_3 , or $\rho=1$ and the total CARS signal I_{CARS} coincides with the so-called Yuratich expression $I_{CARS} = I_1 + I_2 + 2I_3$.⁷ For example, this is exactly what happens far from the Raman resonances, where the susceptibility is rather flat. On the contrary, if χ_{1S} and χ_{2S} cannot be uncoupled in the convolution of I_4 , then $I_4 < I_3$ or $\rho < 1$ and the simpler Yuratich expression cannot be adopted. This means that the ratio $\rho = I_4 / I_3$ can only vary from zero to unity (incoherent limit) and, as a consequence, a value of ρ well below unity signifies that coherence must be considered in the calculation, whereas ρ approaching unity guarantees a certain margin of negligibility of coherent contributions to the total CARS signal I_{CARS} . This margin, which remains unpredictable from the perspective of the traditionally accepted criterion of $\sigma_1 \ll \Gamma_j$, can, in contrast, be quantified by the numerical value of ρ . Therefore, the knowledge of ρ represents an useful piece of information particularly needed in those cases where pump laser linewidths and Raman widths are not so remarkably different. For example, single mode Nd:Yag lasers have linewidths of about 0.003 cm^{-1} whereas molecular widths might be not so much greater than one order of magnitude and the question of whether or not a factor of ten is sufficient to fulfill the condition $\sigma_1 \ll \Gamma_j$ arises. This problem becomes even more relevant when using Nd:Yag lasers with intracavity etalon where the linewidth increases to about 0.1 cm^{-1} , a number that is comparable with molecular widths.

To better investigate this problem, the question of how much I_4 differs from I_3 can only be answered after having assigned the laser profiles. For this reason, a less qualitative discussion about ρ calls for the results given in Eqs. (17) and (21). Regrettably, their ratio is a complicated function taking in mutual influences of neighboring Raman transitions and the analytical reasoning does not go beyond the formal expressions of I_{3g} and I_{4g} . To avoid the recourse to numerical examples for the calculation of ρ , let us explore the possibility of an analytical function that could immediately indicate the physical framework necessary to interpret the CARS data. However, it is obvious that it would be impractical to carry out the present calculation for the entire frequency range determined by the wave mixing of ω_1 , ω_2 and ω_S , nevertheless the search for analytical solutions can still be interesting if restricted to the most important points of a CARS spectrum, that is the spectral peaks corresponding to the Raman transitions found at $\omega_a = \bar{\omega}_{1,2} + \Omega_j$. The additional simplification is that we suppose small perturbations of neighboring Raman levels, in this way the summations of Eqs. (17) and (21) reduce to the j -th peak of the CARS spectrum relative to the chosen j -th resonance frequency, that is

$$I_{3g}^{1S} \cong \frac{1}{2} KL_1 L_2 L_S \frac{1}{\sigma_2 \sqrt{\sigma_1^2 + \sigma_S^2}} \exp[-(\omega_a - \bar{\omega}_a)^2 / \sigma_{12S}^2] a_j^2 \frac{\text{Re}[w(z_j)]}{2\Gamma_j}, \quad (23)$$

$$I_{4g} \cong \frac{1}{2} KL_1 L_2 L_S \frac{\sqrt{\pi}}{\sigma_1 \sigma_2 \sqrt{\sigma_1^2 + \sigma_S^2}} \exp[-(\omega_a - \bar{\omega}_a)^2 / \sigma_{12S}^2] a_j^2 \{ \text{Re}[w(z'_{1,j})] \text{Re}[w(z'_{2,j})] + \text{Im}[w(z'_{1,j})] \text{Im}[w(z'_{2,j})] \}. \quad (24)$$

If we recall the degeneracy of the pump lasers ($\bar{\omega}_1 = \bar{\omega}_2$ and $\sigma_1 = \sigma_2$) and the hypothesis of broadband CARS ($\sigma_S \gg \sigma_1$), we find that $z_j = z'_{1,j} = z'_{2,j} = i\Gamma_j / \sigma_1$ and, as a result, the complex error function loses its imaginary part and $w = \exp[(\Gamma_j / \sigma_1)^2] \text{erfc}[\Gamma_j / \sigma_1]$. This means that the on-resonance ratio ρ_{on} for the j -th CARS peak has then a simple description

$$\rho_{\text{on}} = \sqrt{\pi} \Gamma_j \exp[(\Gamma_j / \sigma_1)^2] \text{erfc}(\Gamma_j / \sigma_1) / \sigma_1, \quad (25)$$

which depends only on the dimensionless ratio between the Raman width Γ_j and the laser bandwidth σ_1 . Under the assumption of largely spaced Raman transitions and degenerate pump lasers, the result in Eq. (25) establishes the quantitative criterion needed to discriminate between the coherent convolution of Eq. (3) and the simpler incoherent spectral synthesis of Eq. (2) [or its ideal limit given in Eq. (1)]. As said before, this choice usually rests on a qualitative approach according to which σ_1 is broadly compared with Γ_j . According to the usual reasoning, if $\sigma_1 \ll \Gamma_j$ (i.e. narrowband pump lasers) the complications associated with Eq. (3) can be dropped and Eq. (1) or (2) is used instead. The drawback of such a criterion is that it is difficult to define the threshold beyond which Eq. (3) can be abandoned in favor of simpler expressions. Conversely, the result in Eq. (25) offers an accurate definition of what has so far been depended on qualitative considerations. In particular, ρ_{on} is shown in Fig. 1 as a function of $\eta_j = \Gamma_j / \sigma_1$ and quantitative evaluations are possible from the numerical values reported in the figure.

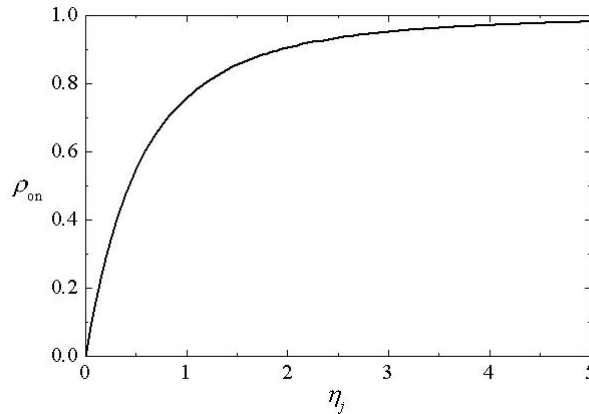


Fig. 1 Behavior of Eq. (25) as a function of the dimensionless ratio $\eta_j = \Gamma_j / \sigma_1$.

For instance, it is found that $\eta_j = 5$ is already a satisfactory threshold to assume the limit of narrowband pump lasers with a margin of more than 98 %. Of course, the more $\eta_j > 5$ and the more ρ_{on} tends to one. For example, let us take $\eta_j = 10$ (which is typical for single mode Nd:Yag lasers and Q-branch CARS spectra³⁹), it is found that the margin of negligibility of coherence increases to about 99.5 % (or $\rho_{\text{on}} \cong 0.995$). As a result, it is acceptable to say that Eq. (25) gives a reasonable explanation of how laser monochromaticity acts in the convolutions of Eq. (3). In particular, if the two spectral components χ_{1S} and χ_{2S} of CARS susceptibility are sufficiently uncoupled, ρ_{on} establishes the goodness of the assumed narrowband limit. In the opposite limit of finite laser bandwidth, ρ_{on} is well below unity and its value determines the importance of the coherent integral (I_{4g}) with respect to the incoherent counterpart (I_{3g}). For instance,

the effect of coherence amounts to about three quarter of I_{3g} ($\rho_{\text{on}} \cong 0.75$) when σ_1 is comparable with Γ_j (note that $\sigma_1 \approx \Gamma_j$ is typical for Nd:Yag lasers with intracavity etalon).

In the derivation of Eq. (25), the assumption of largely spaced Raman resonances sounds as a restriction of a more general treatment where Raman transitions are closely spaced. Apparently, the assumption (necessary to guarantee the analyticity of the result) holds true for molecular hydrogen only. For other molecular constituents that are typical for CARS measurements and showing partial overlap of Raman resonances, the most general solution lies in the direct numerical calculation of I_{3g} and I_{4g} , respectively given in Eq. (17) and (21). As an example, taking the case of vibrational CARS of molecular nitrogen [14] (which is one of the most studied molecules in CARS spectroscopy [1]), it turns out that $\rho_{\text{on}}^{N_2}$ follows the same behavior shown in Fig. 1, except for a slight lift of the curve (for instance, in Fig. 1 $\rho_{\text{on}} = 0.546$ at $\eta_j = 0.5$ while $\rho_{\text{on}}^{N_2} = 0.552$ for the same value of η_j). The upward shift is rather small, actually almost negligible, but it is still indicative that the overlap between Raman transitions acts as if the relevant spectral width was larger than the Raman width Γ_j of a single line. This is easily understandable, because the overlap introduces additional spectral components within which coherence can be established and the whole problem can be viewed as if there was an effective Raman width Γ_j^{eff} greater than Γ_j . As a consequence, the limit of incoherent convolution ($\rho_{\text{on}} \rightarrow 1$) may be reached more easily if overlap of Raman transition occurs.

As a final comment, it is plausible to say that the function contained in Eq. (25) constitutes a useful criterion to determine the actual impact of coherence on CARS data. The relevance of such quantitative criterion is especially strengthened by the criticality in the choice between incoherent and coherent approach in the range $1 \leq \eta_j \leq 10$ where real pump lasers with different line-narrowing mechanisms are situated. It is then undeniable that this criticality cannot be solved by the broadness of the ordinary criterion of $\sigma_1 \ll \Gamma_j$. The knowledge of the analytical function of Eq. (25) could instead help the spectroscopist to decide which approach to choose in analyzing the data, without the uncertainty accompanying the rough comparison between σ_1 and Γ_j .

5. CONCLUSIONS

In summary, a proposal has been formulated to justify qualitative arguments introduced in literature to discriminate between coherent and incoherent convolutions needed in the reconstruction of CARS spectra obtained with the most common laser configuration of two degenerate pump beams.

The result of this work is Eq. (25), which, even though obtained under the hypothesis of largely spaced Raman transitions, suggests a quantitative method of discrimination between the two standard approaches to CARS synthesis. It appears that the classical criterion of $\sigma_1 \ll \Gamma_j$ (laser linewidth much smaller than the Raman width) has now a well-founded explanation in terms of the limit behavior of the mathematical function described in Eq. (25). In addition, it has been shown that a value of ten for the ratio Γ_j / σ_1 is already enough to neglect coherent contributions to the total CARS intensity of molecules with well separated Raman resonances. This is a confirmation of what has been hypothesized in some analysis of CARS experiments employing single-mode Nd:Yag lasers.^{10, 33} On the contrary, experiments where pump laser linewidth is comparable to Γ_j (for example, this holds true for Nd:Yag lasers with intracavity etalon^{15-18, 20-21, 23, 24, 26, 28-32, 36}) are prone to the influence of coherence and a more elaborate analysis is preferable, although some authors have declared the use of simpler solutions.^{16, 20, 23, 24}

Overlap between Raman transitions was excluded in the derivation of the analytical function of Eq. (25). However, it can be demonstrated with numerical examples that a small increase can be expected in the calculation leading to the main result of this paper. This is explainable in terms of a larger spectral width due to the additional frequencies that the overlap entails. Note that the consequence is convenient as it favors the fulfilment of incoherent convolution.

REFERENCES

1. A. C. Eckbreth, *Laser Diagnostics for Combustion Temperature and Species*, p. 281-380, Gordon and Breach Publishers, Amsterdam, 1996.
2. W. Demtröder, *Laser Spectroscopy*, p. 517-522, 553, Springer, Berlin, 2003.
3. W. M. Tolles, J. W. Nibler, J. R. McDonald, A. B. Harvey "A review of the theory and application of coherent anti-Stokes Raman spectroscopy (CARS)", *Appl. Spectr.* **31**, 253-271 (1977).
4. S. A. J. Druet, J. P. E. Taran, "CARS spectroscopy", *Prog. Quant. Electr.* **7**, 1-72 (1981).
5. D. A. Greenhalgh, "Quantitative CARS spectroscopy", in *Advances in non-linear spectroscopy*, ed. by R. J. H. Clark and R. E. Hester, Vol. 15, p. 193-251, John Wiley & Sons, New York, 1988.
6. P. D. Maker, R. W. Terhune, "Study of optical effects due to an induced polarization third order in the electric field strength", *Phys. Rev.* **137**, A801-818 (1965).
7. M. A. Yuratich, "Effects of laser linewidth on coherent anti-Stokes Raman spectroscopy", *Mol. Phys.* **38**, 625-655 (1979).
8. H. Kataoka, S. Maeda, C. Hirose, "Effects of laser linewidth on the coherent anti-Stokes Raman spectroscopy spectral profile", *Appl. Spectr.* **36**, 565-569 (1982).
9. L. A. Rahn, R. L. Farrow, R. P. Lucht, "Effects of laser field statistics on coherent anti-Stokes Raman spectroscopy intensities", *Opt. Lett.* **9**, 223-225 (1984).
10. R. E. Teets, "Accurate convolutions of coherent anti-Stokes Raman spectra", *Opt. Lett.* **9**, 226-228 (1984).
11. R. L. Farrow, L. A. Rahn, "Interpreting coherent anti-Stokes spectra measured with multi-mode Nd:Yag pump lasers", *J. Opt. Soc. Am. B* **2**, 903-907 (1985).
12. D. A. Greenhalgh, R. J. Hall, "A closed form solution for the CARS intensity convolution", *Opt. Comm.* **57**, 125-128 (1986).
13. F. Y. Yueh, E. J. Beiting, "Analytical expressions for coherent anti-Stokes Raman spectral (CARS) profiles", *Comp. Phys. Comm.* **42**, 65-71 (1986).
14. J. C. Luthe, E. J. Beiting, F. Y. Yueh, "Algorithms for calculating coherent anti-Stokes Raman spectra: application to several small molecules", *Comp. Phys. Comm.* **42**, 73-92 (1986).
15. F. Y. Yueh, E. J. Beiting, "Simultaneous N₂, CO and H₂ multiplex CARS measurements in combustion environments using a single dye laser", *Appl. Opt.* **27**, 3233-3243 (1988).
16. M. Aldén, P. E. Bengtsson, H. Edner, S. Kröll, D. Nilsson, "Rotational CARS: a comparison of different techniques with emphasis on accuracy in temperature determination", *Appl. Opt.* **28**, 3206-3219 (1989).
17. S. Kröll, M. Aldén, P. E. Bengtsson, C. Löfström, "Evaluation of precision and systematic errors in vibrational CARS thermometry", *Appl. Phys. B* **49**, 445-453 (1989).
18. R. Bombach, T. Gerber, B. Hemmerling, W. Hubschmid, "Aspects of hydrogen CARS thermometry", *Appl. Phys. B* **51**, 59-60 (1990).
19. R. D. Hancock, P. O. Hedman, S. K. Kramer, "Coherent anti-Stokes Raman spectroscopy (CARS) in coal-seeded flames", *Comb. Flame* **87**, 77-88 (1991).
20. L. Martinsson, P. E. Bengtsson, M. Aldén, S. Kröll, J. Bonamy, "A test of different rotational Raman linewidth models: accuracy of rotational coherent anti-Stokes Raman scattering thermometry in nitrogen from 295 to 1850 K", *J. Chem. Phys.* **99**, 2466-2477 (1993).
21. J. P. Singh, F. Y. Yueh, W. Kao, R. L. Cook, "Study of high-temperature multiplex HCl coherent anti-Stokes Raman spectroscopy spectra", *Appl. Opt.* **32**, 894-898 (1993).
22. V. Bergmann, W. Stricker, "H₂ CARS thermometry in a fuel-rich, premixed, laminar CH₄/air flame in the pressure range between 5 and 40 bar", *Appl. Phys. B* **61**, 49-57 (1995).
23. L. Martinsson, P. E. Bengtsson, M. Aldén, "Oxygen concentration and temperature measurements in N₂-O₂ mixtures using rotational coherent anti-Stokes Raman spectroscopy", *Appl. Phys. B* **62**, 29-37 (1996).
24. R. Fantoni, F. Colao, L. De Dominicis, M. Giorgi, M. D'Apice, S. Giannini, H. J. L. Van der Steen, "On-line nitrogen CARS thermometry on a 130 kW burner by using a neural network approach", *J. Raman Spectr.* **31**, 697-701 (2000).
25. J. Bood, P. E. Bengtsson, T. Dreier, "Rotational coherent anti-Stokes Raman spectroscopy (CARS) in nitrogen at high pressures (0.1-44 MPa): Experimental and modelling results", *J. Raman Spectr.* **31**, 703-710 (2000).
26. J. Bood, P. E. Bengtsson, M. Aldén, "Temperature and concentration measurements in acetylene-nitrogen mixtures in the range 300-600 K using dual-broadband rotational CARS", *Appl. Phys. B* **70**, 607-620 (2000).

27. L. R. Brock, H. G. Adler, "N₂ CARS thermometry within the outer jacket of a metal halide lamp", *Appl. Spectr.* **54**, 918-922 (2000).
28. W. Clauss, V. I. Fabelinsky, D. N. Kozlov, V. V. Smirnov, O. M. Stelmakh, K. A. Vereschagin, "Dual-broadband CARS temperature measurements in hydrogen-oxygen atmospheric pressure flames", *Appl. Phys. B* **70**, 127-131 (2000).
29. F. Beyrau, A. Bräuer, T. Seeger, A. Leipertz, "Gas-phase temperature measurement in the vaporizing spray of a gasoline direct-injection injector by use of pure rotational coherent anti-Stokes Raman scattering", *Opt. Lett.* **29**, 247-249 (2004).
30. V. A. Shakhmatov, O. De Pascale, M. Capitelli, "Theoretical and experimental CARS rotational distributions of H₂ (X¹Σ_g⁺) in a radio-frequency capacitive discharge plasma", *Eur. Phys. J. D* **29**, 235-245 (2004).
31. F. Vestin, M. Afzelius, P. E. Bengtsson, "Improved species concentration measurements using a species-specific weighting procedure on rotational CARS spectra", *J. Raman Spectr.* **36**, 95-101 (2005).
32. V. A. Shakhmatov, O. De Pascale, M. Capitelli, K. Hassouni, G. Lombardi, G. Gicquel, "Measurement of vibrational, gas and rotational temperatures of H₂ (X¹Σ_g⁺) in radio frequency inductive discharge plasma by multiplex coherent anti-Stokes Raman scattering spectroscopy technique", *Phys. Plasmas* **12**, 23504-1 - 23504-10 (2005).
33. R. D. Hancock, K. E. Bertagnolli, R. P. Lucht, "Nitrogen and hydrogen CARS temperature measurements in a hydrogen/air flame using a near-adiabatic flat-flame burner", *Comb. Flame* **109**, 323-331 (1997).
34. R. J. Hall, "CARS spectra of combustion gases", *Comb. Flame* **35** 47-60 (1979).
35. R. J. Hall, "Coherent anti-Stokes Raman spectroscopic modeling for combustion diagnostics", *Opt. Eng.* **22**: 322-329 (1983).
36. L. P. Goss, D. D. Trump, B. G. MacDonald, G. L. Switzer, "10-Hz coherent anti-Stokes Raman spectroscopy apparatus for turbulent combustion studies", *Rev. Sci. Instr.* **54**, 563-571 (1983).
37. W. Koechner, *Solid-State Laser Engineering*, Springer, Berlin, 1999.
38. M. Abramowitz, I. A. Stegun, *Handbook of Mathematical Functions*, p. 297, Dover, New York, 1974.
39. R. J. Hall, "Pressure-broadened linewidths for N₂ coherent anti-Stokes Raman spectroscopy thermometry", *Appl. Spectrosc.* **34**, 700-702 (1980).